Neutrophil-Inspired Zn/ZnO/Cu Core/Shell/Shell Particles for Diabetic Wound Treatment

Guangshun Yi[a], Shujun Gao[b], Xiukai Li[a], Jinquan Wang[a], Siew Ping Teong[a], Shook Pui Chan[a], Hongfang Lu[b], Jackie Y. Ying[b], Yugen Zhang*[a]*

Abstract: *A Zn/ZnO/Cu core/shell/shell particle designed to emulate neutrophils and capable of generating hypochlorous acid has been successfully synthesized and comprehensively examined. Given hypochlorous acid's potent antimicrobial properties, Zn/ZnO/Cu exhibits remarkable effectiveness against both microorganisms and viruses. Its application in diabetic wound healing has been investigated, revealing superior outcomes in comparison to prevalent silver-based commercial products.*

Keywords: Zn/ZnO/Cu · hypochlorous acid · hypohalous acid · antimicrobial · Wound healing

1. Introduction

Hypochlorous acid (HOCl) is one of the most powerful microbicidal agents,[1-3] and it is a natural product produced by human neutrophil cells in response to infections,[4, 5] making it expected to be compatible with the human body. It would be an ideal disinfectant for human in vivo applications such as wound healing. However, HOCl is not stable, and a commercial pharmaceutical formulation containing pure HOCl has not been developed.[1]

Neutrophils are a subtype of white blood cells. Myeloperoxidase, an enzyme in neutrophils, catalyzes the conversion of chloride ions (or hypobromous acid, HOBr, if bromide ions are present) to HOCl in the presence of hydrogen peroxide (H_2O_2), which is self-generated by the respiratory O_2 burst via NADPH oxidase (as shown in Scheme 1).[6] Recently, our group found that zinc oxide-coated zinc (Zn/ZnO core/shell) can generate H_2O_2 and superoxide radicals ($\cdot O_2^-$),[7-9] while certain metals like copper were reported to catalyze the reaction of chloride ions and H_2O_2 to produce HOCl.[10]

Inspired by the mechanism of neutrophils, in this study, we have prepared particles comprising of a zinc core, zinc oxide shell, and copper outer shell (Zn/ZnO/Cu particles, referred to as ZZCP). We have shown that these particles can generate HOCl and possess good antimicrobial and antiviral properties. We have studied the application of ZZCP for diabetic wound healing, and it showed good results with good safety profile.

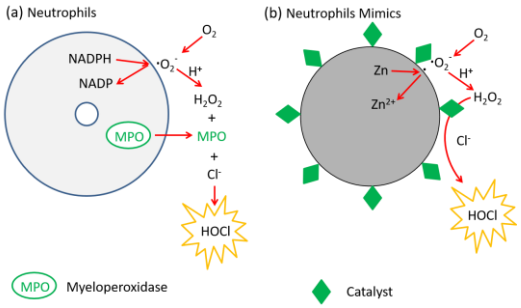

Scheme 1. The generation of HOCl (a) by neutrophils and (b) by Zn/catalyst core/shell particles.

[a] *Institute of Bioengineering and Bioimaging (IBB), 31 Biopolis Way, The Nanos, Singapore 138669, Singapore.*
[a.] *Institute of Sustainability for Chemicals, Energy and Environment (ISCE2), 1 Pesek Road Jurong Island, Singapore 627833. Email: yi_guangshun@isce2.a-star.edu.sg; zhang_yugen@isce2.a-star.edu.sg.*
[c] *NanoBio Lab, Institute of Materials Research and Engineering (IMRE), 31 Biopolis Way, The Nanos, Singapore 13863*

2. Experimental section

2.1 Sample preparation

Preparation of Zn/ZnO/Cu core/shell particles with 1 mol% Cu. Accurately weight 1 g Zn powder (15.3 mmol), mix with 1 ml of 1 wt% HCl in a 15 ml Eppendorf centrifuge tube to remove any ZnO residue. After centrifuge and discard the supernatant, the Zn powder was dispersed in 20 ml water in a 50 ml of glass beaker. In another 15 ml centrifuge tube, 38.18 mg of $CuSO_4.5H_2O$ (0.153 mmol) was dissolved in 10 ml water. Under magnetic stirring at 500 rpm in the beaker, 10 ml $CuSO_4.5H_2O$ solution was added drop by drop. The reaction last for 1 h at room temperature. After reaction, the solution was centrifuged, washed twice with water and once with ethanol, and dried in vacuum oven at 50 °C.

Same as above, Cu/Zn ratio to 0 mol% to 2 mol% was prepared.

Preparation Antimicrobial and antiviral testing surfaces. 0.02 g of powder was added in 100 µl of absolute ethanol in a 2 ml centrifuge tube. After ultrasonic treatment for 30 seconds (VWR 50 T, 50/60 HZ), the suspension was spread onto a 2.5 cm × 2.5 cm glass slide (cut from microscope slide, Marienfeld, Germany). The surface was dried in a 60 °C oven for 1 h before antimicrobial testing.

Preparation of wound healing gauze. Commercial cotton gauze was purchase from Watsons and was cut to 2cm × 1.5cm before use. Accurately weigh 0.01 g Zn/ZnO/Cu particles and dispersed in 200 µl of absolute ethanol. After sonicate for 30 seconds, 100 µl of suspension was taken with a pippete and spread evenly onto the gauze, repeat this step for the rest of 100 µl suspension. The gauze was dried in air and further UV sanitized for 20 min in a BSC before wound healing study.

2.2 HOX detection and durability test

HOCl detection by phenol red assay: In a 15 ml phenol red solution (5×10^{-5} M) containing 0.025M NaCl, 10 mg ZZCP was added. Under magnetic stirring at 1000 rpm, wait for red color solution became colorless. The generation of HOCl was further confirmed by HOCl scavengers with either 3-amino-1,2,4-triazole (AT) or taurine (Tau) in the phenol red degradation reaction (1 mM).

HOBr and HOI detection by phenol red assay: Same as above, but change NaCl to NaBr and NaI, respectively.

HOCl scavenger quenching experiments. 3-amino-1,2,4-triazole (AT) was used as scavenger for HOCl/OCl^-. To prove the production of HOCl, four samples of A-D was prepared. Each sample containing 15 ml phenol red solution (5×10^{-5} M) and 0.025M NaCl, other component in each sample are: A. none; B: AT (1 mM, 1.26 mg); C: 10 mg ZZCP; and D: 10 mg ZZCP with AT (1 mM, 1.26 mg). The four samples were stirring at 1000 rpm in open air, until colorless.

HOCl detection by celestine blue (CB) assay: 10 mg of ZZCP was added to 10 mL of CB solution in water (1×10^{-4} M), in the absence and presence of 10 mM Cl^-. Magnetic stirring was carried out at 1000 rpm. The solution with Cl^- gradually turned pink, while the CB solution without Cl^- remained dark blue during the reaction, further confirming that ZZCP can convert Cl^- into HOCl.

2.3 Biological experiments

Antimicrobial testing (JIS Z 2801/ISO 22196 method).[11] Before the testing, *E. coli* and *S. aureus* were adjusted to OD_{600} = 0.07 in TSB, and *C. albicans* in YMB. This corresponds to 3×10^8 CFU/ml. The solution was further diluted 100 times in TSB or YMB and 100 µL of cell suspensions was placed on the testing surfaces. After covering with a 2 cm × 2 cm polyethylene covering film, the testing surface was incubation for 24 h at 37 ºC (for *E. coli* and *S. aureus*) and room temperature for *C. albicans*. Cells on the testing surface were washed off with 9.9 ml of pH 7.4 PBS buffer solution, sequentially diluted and plated on 1.5 % LB agar plates. Resulting colonies were counted using standard plate count techniques, and the number of colonies forming units (CFU) per mL was calculated.

Antivirus test against Phages (ISO 27102 method).[12] Stock solutions of bacteriophages of MS2 and phi6 or mouse hepatitis virus (MHV) were serially diluted to obtain a working concentration, and 100 uL of the solution was introduced onto the testing surfaces measuring 2.5 cm by 2.5 cm square. The droplet was immediately covered with a plastic polyethylene sheet measuring 2 cm by 2 cm, and the samples were then incubated at 35 °C (for phi6) or at room temperature (for MS2 and MHV). After a predetermined incubation time (18 h for MS2 and phi6, and 4 h for MHV), viable phages and MHV were recovered and determined by the number of plaque forming units, and PFU per mL (PFU/ml) was then calculated. Detailed protocol please find in the supporting information.

Diabetic wound healing study

Diabetes mellitus was induced chemically according to a literature method.[13, 14] Briefly, after a 12-h fast, rats received a single intraperitoneal injection of streptozotocin (65 mg/kg, merck chemical, Darmstadt, Germany) freshly prepared in 0.1 M sodium citrate buffer (pH 3.4). At 8 d after streptozotocin injection, blood glucose measurement was performed on tail-vein blood by using a glucometer (Accu Chek, Roche Diabetes Care, Singapore). Rats whose fasting blood glucose levels exceeded 250 mg/dL (13.8 mmol/dL) were considered diabetic. To confirm the diabetic state, fasting blood glucose measurement was repeated on the day of euthanasia.

Wound healing study. The infected wound model was made by two main steps: i) removal of a full thickness of skin (Ø0.8cm) on the part of rat dorsal thoracic with the biopsy punch; ii) introduction of 100 µL of SA suspension (1 × 10^6 CFU mL^{-1}) and incubation for 30 minutes. After that, blank gauze, gauze embedded with ZZCP, and commercial UrgoTul® Silver gauze was applied onto the infected wound topically. The wound size was monitored and measured.

3. Results and discussion

3.1 Synthesis, characterization, and optimization

The ZZCP were synthesized via a simple room temperature reaction in water between Zn and Cu^{2+}. Before the reaction, smooth Zn surfaces were observed, as shown in Figure 1a. However, after reaction with 1 mol% of Cu^{2+}, plate-like particles were grown on the Zn surface (Figure 1b). Elemental maps for Zn, O, and Cu for the particles in Figure 1b are shown in Figures 1c to 1e. To determine the exact composition of the final product, we prepared products with various Cu^{2+}/Zn molar ratios of 1% (Figure 1b), 10% (Figure 1f), and 100% (Figure 1g), and characterized them by SEM and XRD.

From 1% to 10% Cu^{2+}/Zn molar ratios, more and more small round-shaped nanoparticles appeared and adhered to the plate-like particles, most likely Cu nanoparticles. When the Cu^{2+}/Zn molar ratio increased to 100% (Figure 1g), the big particles collapsed, leaving only the plate-shaped particles and small round-shaped nanoparticles, suggesting the disappearance of Zn and the formation of ZnO plates and Cu nanoparticles. This was confirmed by XRD in Figure 1h. When the Cu^{2+}/Zn ratio was increased from 0% to 1 mol%, the diffraction peak of Zn showed a minor intensity decrease, indicating that some Zn was lost through the reaction of $Zn + Cu^{2+} = Zn^{2+} + Cu$. When the Cu^{2+}/Zn ratio was further increased to 100 mol%, the diffraction peak of Zn disappeared, and new diffraction peaks of wurtzite ZnO appeared, indicating the full consumption of Zn and the formation of ZnO.

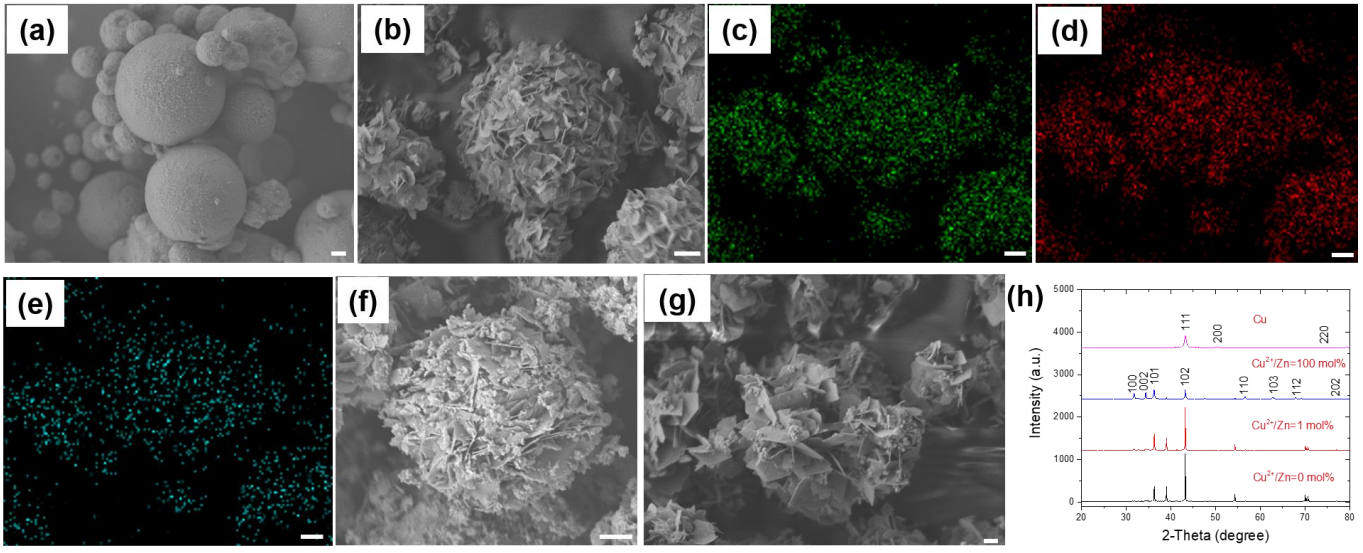

Figure 1. (a) SEM image of Zn particles, (b) SEM images of the product prepared with Cu^{2+}/Zn=1 mol% in water, (c-e) Elemental mapping of the product for Zn (c), O (d), and Cu (e), respectively. (f-g) SEM images of the product prepared with Cu^{2+}/Zn=10 mol% and 100%. (h) displays the XRD diffraction pattern for products prepared with various Cu^{2+}/Zn ratios. Bar = 1 µm.

The obtained product appeared as black powder after drying. When HCl was added, it partially dissolved and formed a colorless transparent supernatant and a brownish precipitate (black in water and brown color when dry, Figure S1). XRD confirmed that the brown precipitate was copper metal (Cu), while the supernatant solution was confirmed to be a Zn^{2+} solution, as when NaOH solution was added to the transparent supernatant solution, a white precipitate formed, which was confirmed by XRD to be ZnO after drying in oven (Figure S1). We also confirmed by SEM that after HCl dissolving, only nanoparticles remained, as the plate-like particles had disappeared. Based on this information, we confirm that the product in Figure 1b has a Zn/ZnO/Cu core/shell/shell structure.

3.2 Proof-of-concept for HOCl

The generation of HOCl was first demonstrated through a series of phenol red chlorination/degradation reactions by ZZCP, in the presence or absence of Cl^-. Figure 2a shows that phenol red (PR) can react with HOCl to form chlorophenol red ($PRCl_2$).[15] In Figure 2b, a 5×10^{-5} M PR aqueous solution was mixed with ZZCP, with and without Cl^-. Without Cl^-, the solution remained red with no apparent color change during the 2.5-hour reaction. However, upon addition of 1×10^{-3} M Cl^-, the PR gradually shifted to a purple color before completely degrading into a colorless solution. The pH of all solutions remained constant at pH 7 throughout the reaction. At this pH, PR is red while $PRCl_2$ is purple (Figure S2), indicating that the color change was due to the release of HOCl, as proposed in Scheme 1, followed by the formation of $PRCl_2$. HOCl played two roles in the reaction: chlorination of PR and/or degradation/bleaching of PR. Notably, at pH 7, HOCl and OCl^- coexist, with approximately 70% being HOCl and 30% being OCl^-.[16]

The formation of HOCl was further confirmed through scavenger reactions with two well-known HOCl scavengers: 3-Amino-1,2,4-triazole (AT)[10] and taurine (Tau)[17-19]. Figure 2c and 2d show PR in a 25 mM aqueous Cl^- solution mixed with ZZCP (1 mol% Cu), appearing red at pH 7. The solution on the left had no scavenger, while the middle and right solutions were mixed with 1 mM AT and 1 mM Tau, respectively. After 1 hour, the solution without an HOCl scavenger had completely degraded into a colorless solution (becoming colorless at approximately 40 minutes), whereas the solutions with AT or Tau remained red. This suggests that the presence of HOCl scavengers significantly slowed down the PR degradation/bleaching reaction. Additionally, the degradation rate increased with increasing Cl^- concentration (Figure S3); for instance, with 1 mM Cl^- (Figure 2b), complete degradation occurred at 3 hours, while with 25 mM Cl^- (Figure 2c-2d), complete degradation occurred in less than 1 hour. It was also found that AT completely quenched HOCl, while Tau only partially quenched HOCl.

Lastly, the generation of HOCl was also confirmed through celestine blue oxidation reactions by $HOCl^3$ from ZZCP, in the absence and presence of Cl^-. Figure 2e-2f and Figure S4a shows that a 10 mL celestine blue solution in water was mixed with 10 mg of ZZCP. The solution on the left had no Cl^-, while the solution on the right contained 10 mM Cl^-. The solution with Cl^- gradually turned pink while the celestine blue solution without Cl^- remained dark blue during the reaction, further confirming that ZZCP particles can

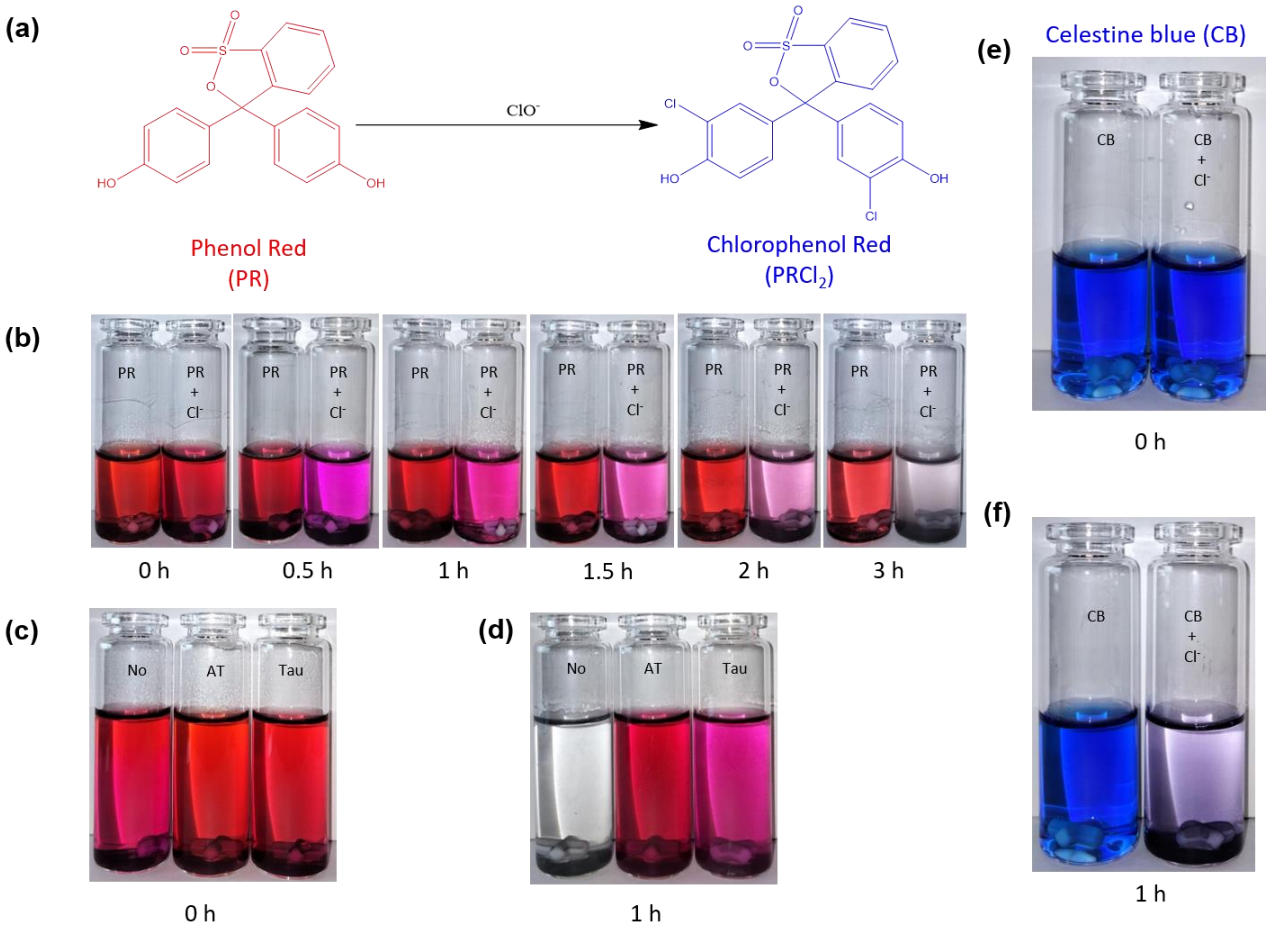

Figure 2. Proof-of-concept for the generation of HOCl by Zn/ZnO/Cu (1 mol% Cu) (a) illustration of phenol red (PR) chlorination by HOCl to form chlorophenol red ($PRCl_2$). (b) PR chlorination/degradation by Zn/ZnO/Cu in the absence and presence of 1 mM Cl^-. (c-d) PR degradation (bleaching) in 25 mM aqueous Cl^- solution by Zn/ZnO/Cu for 1 hour with: no scavenger (left), scavenger 3-Amino-1,2,4-triazole (AT, middle) and scavenger taurine (Tau, right). The presence of an HOCl scavenger significantly delayed PR degradation/bleaching. The pH of all the solution was measured to be 7. At pH7, PR is red, while $PRCl_2$ is purple. Conditions: PR solution (5×10^{-5} M) 9 ml for (b) and 15 ml for (c-d), 10 mg Zn/ZnO/Cu, stir at 1000 rpm. (e-f) celestine blue (CB) oxidation by Zn/ZnO/Cu in the absence and presence of 10 mM Cl^-. Conditions: 10 ml CB solution (5×10^{-5} M), 10 mg Zn/ZnO/Cu, stir at 1000 rpm.

convert Cl^- into HOCl, as suggested in Scheme 1.

3.3 Optimization, antimicrobial and antiviral properties

To determine the optimal formulation of ZZCP, various samples were prepared with different Cu^{2+}/Zn molar ratios ranging from 0% to 2%. The degradation rate of these samples was recorded and compared. As shown in Figure S5a, the presence of Cu with Zn significantly increased the dye degradation capability compared to bare Zn. Cu content ranging from 0.1 to 0.9 mol% demonstrated good performance, with 0.2-0.4 mol% Cu exhibiting the best overall performance.

In addition to converting Cl^- into HOCl, ZZCP can also convert Br^- and I^- into HOBr and HOI, respectively. Figure S5b-5c show that when Br^- and Cl^- are present, a similar dye degradation profile is observed as compared to Cl-.

As ZZCP can convert Cl^- to HOCl, and neutrophil cells in our body release HOCl to defend bacterial and virus infection. The antimicrobial properties and antivirus properties of ZZCP were evaluated. Briefly, 0.02 g of ZZCP (0.4 mol% Cu) was coated onto a 2.5 cm × 2.5 m glass slides, and the antimicrobial properties of the surface was evaluated by JIS Z 2801/ISO 22196 method.[11] As showed in Figure 5, a-c, after 24 hours incubation, ZZCP killed all the *E. coli* (Gram negative bacteria), *S. aureus* (Gram positive bacteria), and *C. albicans* (fungus).

Similarly, the anti-virus properties of ZZCP were also evaluated by ISO 21702 method.[12] Since it is challenging to conduct virus studies with lethal viruses such as SARS-CoV-2 (which require BSL3 or BSL4 laboratories), we used bacteriophages of MS2, phi6, and mouse hepatitis virus (MHV) as viral surrogates for testing.[20] MS2 is a non-enveloped ssRNA bacteriophage that can be tested under BSL2 conditions,[21] while Phi6 is an enveloped dsRNA bacteriophage commonly used as a surrogate for Ebola virus.[22, 23] MHV is another enveloped virus recommended as a viral surrogate for coronavirus.[24, 25] As shown in Figure 5, d-f, after 18 hours (phages) and 4 hours (MHV) incubation, both phages and MHV were completely killed. This showed that ZZCP not only have good antimicrobial properties, it also have good antiviral property.

3.4 Hemolysis, cytotoxicity profiles of ZZCP and application for wound healing.

Since HOCl is a natural product produced by human neutrophil cells to fight infections,[16] it is expected to be compatible with the human body. Given that body fluids contain high concentrations of Cl^- and ZZCP has the ability to convert Cl^- to HOCl, a possible application of ZZCP is to integrate it into cotton gauze to fight infections and accelerate wound healing. However, for in vivo applications, biocompatibility and cytotoxicity of ZZCP is still unknow. Therefore, hemolysis and cytotocixity of ZZCP have been studied.[26, 27] The hemolytic acitivity of ZZCP was examined by incubating ZZCP solution with rat red blood cells (rRBCs) for 1 h. Absorbance of wells with rRBCs lysed with 0.2% Triton X-100 was taken as 100% hemolysis. As shown in Figure 4a, nearly zero hemolytic activity was observed for ZZCP, which suggested that ZZCP did not lead to blood cell hemolysis. The *in vitro* cytotoxicity of ZZCP was studied by the MTT method with L929 mouse fibroblast cells.[26, 28] As shown in Figure 4b, when increase the ZZCP concentration to 20 mg/ml, no obvious cell viability decrease was observed, indicating ZZCP has very low cytotoxicity with mammalian cells.

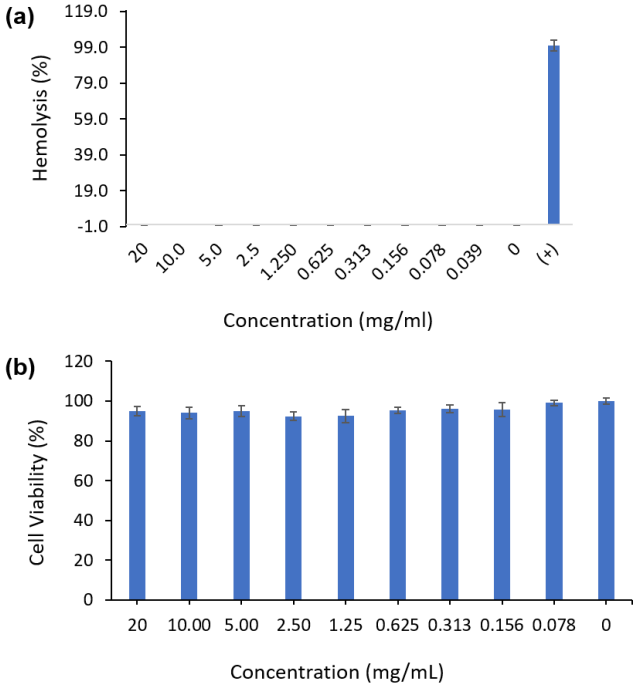

Figure 4. Hemolysis and cytotoxicity test results of ZZCP. (a) Hemolysis of rRBCs after 1 h of incubation with ZZCP and positive control (+): 0.2% Triton X-100. (b) Cell viability of L929 mouse fibroblasts incubated for 24 h for ZZCP at different concentrations. Data are expressed as mean ± S.D. of triplicates.

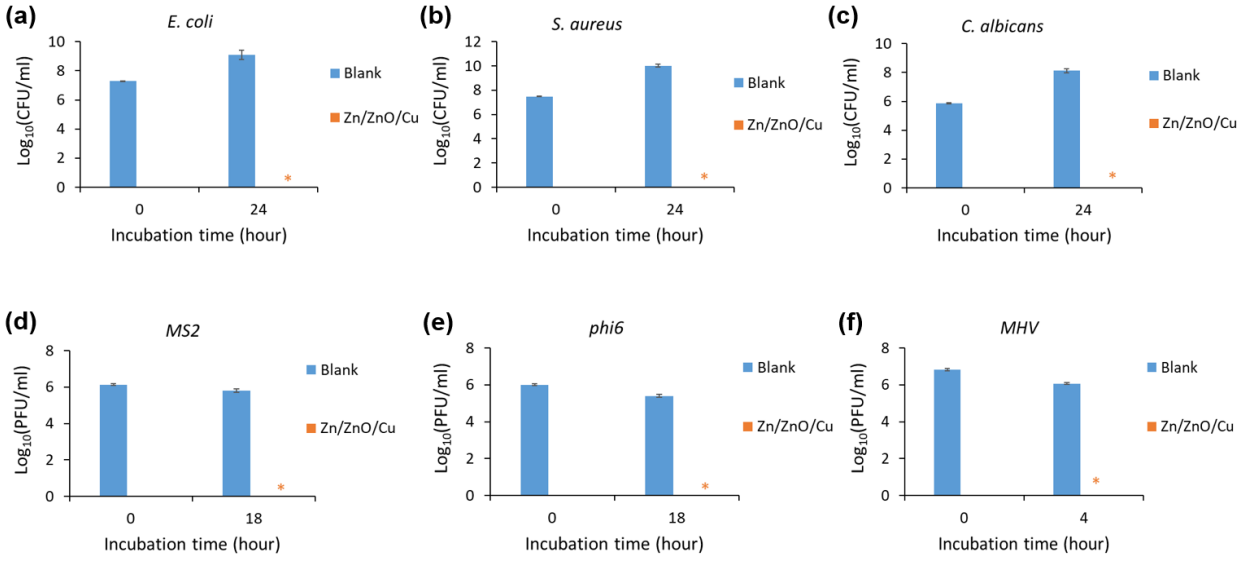

Figure 3. Antimicrobial property (a-c) and antivirus property (d-f) of Zn/ZnO/Cu. * Represents no colony observed.

Singapore is currently experiencing a rising epidemic of diabetes mellitus, and one of the most common complications of this disease is diabetic foot ulcers. Approximately 58% of ulcers often become infected,[29] which can lead to amputation. Unlike normal wounds, diabetic wounds do not follow a typical healing process, and bacterial infection can further disrupt this process.[30] There is a need for innovative topical antimicrobial therapies to aid in the multimodal treatment of these infections.[31] The use of ZZCP for diabetic wound healing has been studied. Cotton gauze (2 cm × 1.5 cm) embedded with ZZCP was applied to wounds, with blank gauze and commercial Ag-coated gauze (UrgoTul® Silver gauze) used as controls. The wounds were created on diabetic rats and further infected with *S. aureus*, and the gauze were applied to treat the wounds.

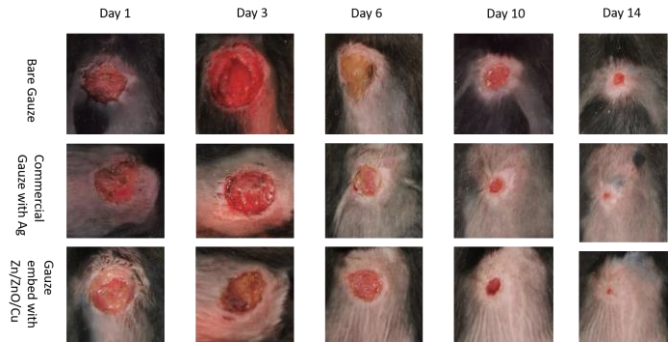

Figure 5. (a-b) S. aureus infected diabetic wounds after treatment with the blank gauze, UrgoTul Silver gauze and gauze load with ZZCP.

As shown in Figures 5, bare gauze showed the obvious slower healing speed. It exhibited an initial worsen of wound in the first 3 days, followed by slowly wound healing. This may due to the wound infection by S. aureus. Compared with bare gauze, commercial gauze with Ag and gauze with ZZCP showed obvious faster wound healing speed at the 3 days. Of the 3 gauzes, gauze embedded with ZZCP give the overall best wound healing speed, followed by UrgoTul Silver gauze and bare gauze.

4. Conclusions

In summary, Zn/ZnO/Cu core/shell/shell particles has been prepared in aqueous solution. It behaves like neutrophils and convert Cl^- to HOCl. It showed good antimicrobial and antivirus properties. Gauze loaded with Zn/ZnO/Cu has better diabetic wound healing power as compared with blank gauze and commercial UrgoTul (R) Silver gauze.

Conflicts of interest

There are no conflicts to declare.

Acknowledgements

This work was supported by the Institute of Bioengineering and Nanotechnology, Biomedical Research Council, Agency for Science, Technology and Research, and National Research Foundation (NRF), the Prime Minister's Office, Singapore under its NRF Competitive Research Program (NRF-CRP19-2017-02).

References

1. M. P. Eryilmaz, I,M,;, Hypochlorous Acid - Analytical Methods and Antimicrobial Activity, *Tropical Journal of Pharmaceutical Research*, 2013, **12**, 4.
2. N. Hatanaka, M. Yasugi, T. Sato, M. Mukamoto and S. Yamasaki, Hypochlorous acid solution is a potent antiviral agent against SARS-CoV-2, *J. Appl. Microbiol.*, 2022, **132**, 1496-1502.
3. Y. Long, L. Li, T. Xu, X. Wu, Y. Gao, J. Huang, C. He, T. Ma, L. Ma, C. Cheng and C. Zhao, Hedgehog artificial macrophage with atomic-catalytic centers to combat Drug-resistant bacteria, *Nat. Commun.*, 2021, **12**, 6143.
4. C. C. Winterbourn, M. B. Hampton, J. H. Livesey and A. J. Kettle, Modeling the reactions of superoxide and myeloperoxidase in the neutrophil phagosome: implications for microbial killing, *The Journal of biological chemistry*, 2006, **281**, 39860-39869.
5. W. Wang, Y. Gao, M. Zhang, Y. Li and B. Z. Tang, Neutrophil-like Biomimic AIE Nanoparticles with High-Efficiency Inflammatory Cytokine Targeting Enable Precise Photothermal Therapy and Alleviation of Inflammation, *ACS Nano*, 2023, **17**, 7394-7405.
6. S. J. Klebanoff, Myeloperoxidase, *Proc. Assoc. Am. Physicians*, 1999, **111**, 383-389.
7. G. Yi, X. Li, Y. Yuan and Y. Zhang, Redox active Zn/ZnO duo generating superoxide (˙O2−) and H2O2 under all conditions for environmental sanitation, *Environmental Science: Nano*, 2019, **6**, 68-74.
8. G. Yi, G. Agarwal and Y. Zhang, ZnO Nanocrystal Coated Zinc Particles Degrade Dyes in the Dark by Constantly Releasing ·O2– and H2O2, *J. Phys. Chem. C*, 2019, **123**, 19230-19237.
9. G. Yi, Y. Yuan, X. Li and Y. Zhang, ZnO Nanopillar Coated Surfaces with Substrate-Dependent Superbactericidal Property, *Small*, 2018, **14**, e1703159.
10. K. Frenkel, F. Blum and W. Troll, Copper ions and hydrogen peroxide form hypochlorite from NaCl thereby mimicking myeloperoxidase, *J. Cell. Biochem.*, 1986, **30**, 181-193.
11. ISO-22196, Measurement of antibacterial activity on plastics and other non-porous surfaces.*Journal*, 2011, DOI: ICS 07.100.10, 15.
12. ISO-21702, Measurement of antiviral activity on plastics and other non-porous surfaces.*Journal*, 2019, DOI: ICS 83.080.01, 20.
13. J. J. Mendes, C. I. Leandro, D. P. Bonaparte and A. L. Pinto, A rat model of diabetic wound infection for the evaluation of topical antimicrobial therapies, *Comp. Med.*, 2012, **62**, 37-48.
14. C. Poblete Jara, G. Nogueira, J. Morari, T. P. do Prado, R. de Medeiros Bezerra, L. A. Velloso, W. Velander and E. P. de Araújo, An older diabetes-induced mice model for studying skin wound healing, *PLoS One*, 2023, **18**, e0281373.
15. G. T. Höfler, A. But and F. Hollmann, Haloperoxidases as catalysts in organic synthesis, *Org. Biomol. Chem.*, 2019, **17**, 9267-9274.
16. L. Wang, M. Bassiri, R. Najafi, K. Najafi, J. Yang, B. Khosrovi, W. Hwong, E. Barati, B. Belisle, C.

Celeri and M. C. Robson, Hypochlorous acid as a potential wound care agent: part I. Stabilized hypochlorous acid: a component of the inorganic armamentarium of innate immunity, *Journal of burns and wounds*, 2007, **6**, e5-e5.
17. S. J. Weiss, R. Klein, A. Slivka and M. Wei, Chlorination of taurine by human neutrophils. Evidence for hypochlorous acid generation, *J. Clin. Invest.*, 1982, **70**, 598-607.
18. J. Marcinkiewicz, A. Grabowska, J. Bereta and T. Stelmaszynska, Taurine chloramine, a product of activated neutrophils, inhibits in vitro the generation of nitric oxide and other macrophage inflammatory mediators, *J. Leukoc. Biol.*, 1995, **58**, 667-674.
19. J. M. Dypbukt, C. Bishop, W. M. Brooks, B. Thong, H. Eriksson and A. J. Kettle, A sensitive and selective assay for chloramine production by myeloperoxidase, *Free Radical Biology and Medicine*, 2005, **39**, 1468-1477.
20. J. Bae and K. J. Schwab, Evaluation of Murine Norovirus, Feline Calicivirus, Poliovirus, and MS2 as Surrogates for Human Norovirus in a Model of Viral Persistence in Surface Water and Groundwater, *Applied and Environmental Microbiology*, 2008, **74**, 477-484.
21. C. Liu, X. Xie, W. Zhao, N. Liu, P. A. Maraccini, L. M. Sassoubre, A. B. Boehm and Y. Cui, Conducting Nanosponge Electroporation for Affordable and High-Efficiency Disinfection of Bacteria and Viruses in Water, *Nano Lett.*, 2013, **13**, 4288-4293.
22. B. Ma, Y. S. Linden, P. M. Gundy, C. P. Gerba, M. D. Sobsey and K. G. Linden, Inactivation of Coronaviruses and Phage Phi6 from Irradiation across UVC Wavelengths, *Environmental Science & Technology Letters*, 2021, **8**, 425-430.
23. N. Aquino de Carvalho, E. N. Stachler, N. Cimabue and K. Bibby, Evaluation of Phi6 Persistence and Suitability as an Enveloped Virus Surrogate, *Environ. Sci. Technol.*, 2017, **51**, 8692-8700.
24. G. M. String, M. R. White, D. M. Gute, E. Mühlberger and D. S. Lantagne, Selection of a SARS-CoV-2 Surrogate for Use in Surface Disinfection Efficacy Studies with Chlorine and Antimicrobial Surfaces, *Environmental Science & Technology Letters*, 2021, **8**, 995-1001.
25. G. Pereira Oliveira and E. G. Kroon, Mouse hepatitis virus: A betacoronavirus model to study the virucidal activity of air disinfection equipment on surface contamination, *J. Virol. Methods*, 2021, **297**, 114274.
26. S. Liu, R. J. Ono, H. Wu, J. Y. Teo, Z. C. Liang, K. Xu, M. Zhang, G. Zhong, J. P. Tan, M. Ng, C. Yang, J. Chan, Z. Ji, C. Bao, K. Kumar, S. Gao, A. Lee, M. Fevre, H. Dong, J. Y. Ying, L. Li, W. Fan, J. L. Hedrick and Y. Y. Yang, Highly potent antimicrobial polyionenes with rapid killing kinetics, skin biocompatibility and in vivo bactericidal activity, *Biomaterials*, 2017, **127**, 36-48.
27. G. Yi, S. Gao, H. Lu, W. Z. Khoo, S. Liu, S. Chng, Y. Y. Yang, J. Y. Ying and Y. Zhang, Surface Antimicrobial Treatment by Biocompatible, Vertically Aligned Layered Double Hydroxide Array, *Adv. Mater. Interfaces*, 2022, **9**, 2101872.
28. R. Villa, C. R. Ortiz, S. Tapia, G. Gonzalez, E. Trillo, K. M. Garza, S. W. Stafford and L. E. Murr, In vitro biocompatibility studies of fibroblast cells on Ti-Ta alloys, *Mater. Trans.*, 2002, **43**, 2991-2994.
29. L. Prompers, M. Huijberts, J. Apelqvist, E. Jude, A. Piaggesi, K. Bakker, M. Edmonds, P. Holstein, A. Jirkovska, D. Mauricio, G. R. Tennvall, H. Reike, M. Spraul, L. Uccioli, V. Urbancic, K. Van Acker, J. Van Baal, F. Van Merode and N. Schaper, Optimal Organization of Health Care in Diabetic Foot Disease: Introduction to the Eurodiale Study, *The International Journal of Lower Extremity Wounds*, 2007, **6**, 11-17.
30. I. G. Gvazava, M. V. Karimova, A. V. Vasiliev and E. A. Vorotelyak, Type 2 Diabetes Mellitus: Pathogenic Features and Experimental Models in Rodents, *Acta Naturae*, 2022, **14**, 57-68.
31. J. Y. Ji, D. Y. Ren and Y. Z. Weng, Efficiency of Multifunctional Antibacterial Hydrogels for Chronic Wound Healing in Diabetes: A Comprehensive Review, *Int J Nanomedicine*, 2022, **17**, 3163-3176.

Table of Contents

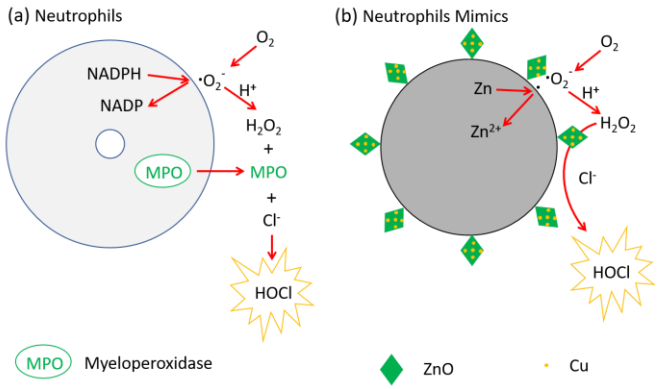

Neutrophil-mimics of Zn/ZnO/Cu core/shell/shell particles have been prepared and proved to produce hypohalous acid in situ. It produce HOCl by first generate $\cdot O_2^-$ and H_2O_2 via electron donation from Zn to O_2, followed by catalytic conversion of Cl^- and H_2O_2 to HOCl via copper. These particles showed good antimicrobial property, antiviral property and biocompatibility profile. Application of Zn/ZnO/Cu for diabetic wound healing were also demonstrated.